

Influence of calcination temperature of TiO₂ nanowires via hydrothermal method for photocatalytic degradation

S. S. Yang^a, B. H. Ren^a, S. Y. Chen^a, S. N. Liu^a, Y. C. Zhang^a, Y. Sun^{a, b, ·}

^a School of Mechanical Engineering, Chengdu University, Chengdu, 610106, China

^b Sichuan Province Engineering Technology Research Center of Powder Metallurgy, Chengdu, 610106, China.

TiO₂ nanowires were prepared by hydrothermal method using tetrabutyl titanate as raw material and then calcined at various temperatures. The samples were characterized by X-ray diffractometer (XRD), scanning electron microscope (SEM) and transmission electron microscope (TEM). The photocatalytic performance of TiO₂ was analyzed by the degradation of Rhodamine B (RhB). The formation mechanism of TiO₂ nanowires was revealed in this study. The results showed that the calcination temperature had a great influence on the crystal structure and morphology of TiO₂ nanowires. The TiO₂ sample calcined at 650 °C exhibited higher photocatalytic activity due to the enhanced crystallinity and the nanowire structure with large specific surface area. As the calcination temperature exceeded 650 °C, the nanowire structure collapsed, leading to a decrease in the photocatalytic degradation efficiency.

(Received October 27, 2022; Accepted January 11, 2023)

Keywords: TiO₂ nanowires, Hydrothermal method, Calcination temperature, Photocatalytic degradation

1. Introduction

Dye pollution in water resources has harmed both human health and the surrounding natural system, which is considered to be a critical problem [1, 2]. It is well known that photocatalytic technology is an effective method to reduce dye pollutant from the wastewater [3-5]. Due to the advantages of high activity, non-toxicity, chemical stability and low price, TiO₂ has been regarded as one of the most promising photocatalysts. However, some limitations prohibit the wider application of TiO₂, including the rapid combination of photogenerated electron-hole pairs and low light harvesting [6-8]. One-dimensional (1 D) TiO₂ structure, such as nanowires, nanotubes and nanorods, has attracted a great deal of research interest due to its large specific surface area and high charge carrier mobility [9-11], which is beneficial to improve the photocatalytic activity. Recently, a number of synthesis methods have been reported to prepare one-dimensional TiO₂ nanomaterials, such as hydrothermal method, template-assisted method, electrochemical anodization and electrospinning [12-15]. Especially, hydrothermal method is easy to control the shape and size of the TiO₂ [16-20] and has been widely investigated. In the previous studies, Guo et al. [21] synthesized TiO₂ nanotubes using P25 as the precursor by hydrothermal treatment, which showed 91.8% degradation efficiency of RhB after 60 min irradiation. Qi et al. [22] have successfully prepared anatase TiO₂ nanorods arrays on ITO conductive film by a hydrothermal process and the degradation efficiency reached 97.9% after 2 h photocatalytic reaction.

In this study, TiO₂ nanowires were synthesized via hydrothermal method using tetrabutyl titanate as the precursor. The growth mechanism of TiO₂ nanowires was proposed by XRD and EDS analysis. The effect of calcination temperature on the crystal structure, morphology and photocatalytic activity of TiO₂ nanowires has been investigated systematically.

· Corresponding author: sunyan@cdu.edu.cn

<https://doi.org/10.15251/DJNB.2023.181.47>

2. Experimental

2.1. Chemical and reagents

Hydrochloric acid (HCl), tetrabutyl titanate (TBT), sodium hydroxide (NaOH) and Rhodamine B were purchased from Kelong chemical company in Chengdu. All water used in the experiment was deionized water.

2.2. Preparation of TiO₂ nanowires

In a typical synthesis, 8 mL of TBT was dissolved into 16 mL of ethanol. Then 6 mL of NaOH solution with a concentration of 10 mol/L was added slowly into the mixed solution by vigorous stirring. The suspension was moved into a 50 mL Teflon-lined autoclave by hydrothermal treatment at 180 °C for 24 h. After that, the filtered product was washed repeatedly with 0.1 mol/L HCl solution and deionized water. The as-prepared samples were obtained by drying at 80 °C for 6 h. Finally, the samples were calcined in a muffle furnace at different temperatures from 450 °C to 950 °C for 2 h.

2.3. Characterization

Crystal structure of the samples was characterized by using an X-ray diffractometer (DX-2700B, China) with Cu K α radiation. Surface morphology and structure were observed by scanning electron microscopy (SEM, S4800, Hitachi). High resolution transmission electron microscopy images were carried out via a FEI Tecnai G2 F20 microscope operated at 120 kV.

2.4. Photocatalytic measurement

The photocatalytic activity of the TiO₂ was evaluated by exploring the degradation of RhB solution with the irradiation of a 350 W Xenon lamp. 100 mg of the TiO₂ was dispersed into 200 mL of RhB solution (10 mg/L) and stirred in the dark for 30 min to obtain the adsorption-desorption equilibrium. At regular time intervals, the concentration of the RhB was calculated by recording the absorbance on the UV-vis spectrophotometer (UV-6100A). The degradation efficiency of RhB was calculated using the formula [23]:

$$\eta(\%) = \frac{C_0 - C}{C_0} = \frac{A_0 - A}{A_0}$$

where C_0 and C are initial concentration and actual concentration of RhB dye at irradiation time t , respectively.

3. Results and discussion

3.1. Structure and phase analysis

To analyze the role of the acid washing process, the XRD of the intermediate product after HCl treatment was performed. As shown in Fig. 1, the main diffraction peaks at $2\theta = 25.3^\circ$ and 48.6° are matched well with H₂Ti₈O₁₇ (PCPDF # 36-0656) [24, 25], which indicates that the hydrothermal product has converted to titanitic acid after acid washing process.

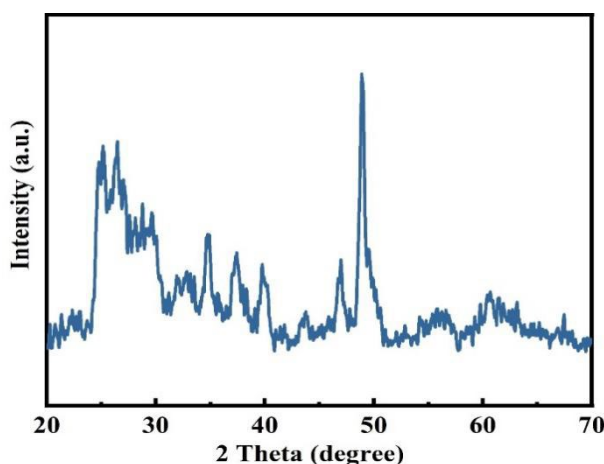


Fig. 1. XRD pattern of the sample after acid washing with HCl.

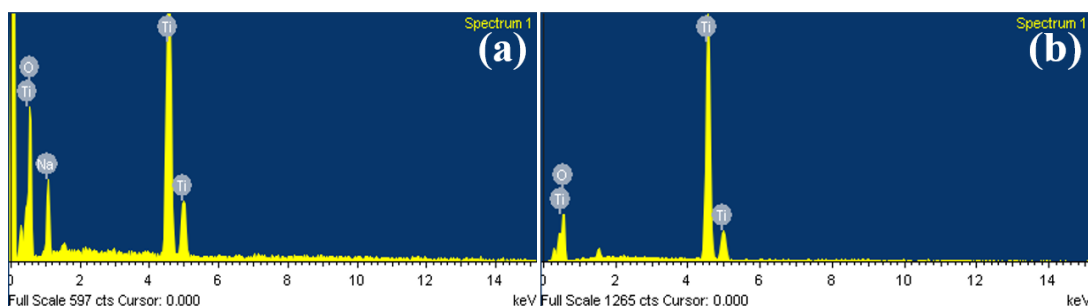


Fig. 2. EDS spectra of samples: (a) after hydrothermal treatment; (b) after calcination at 450°C.

To further investigate the growth mechanism of TiO₂ nanowires, the EDS spectra of the hydrothermal product and the sample calcined at 450°C were carried out. As shown in Fig. 2a, the peaks of sodium (Na), titanium (Ti) and oxygen (O) elements could be observed in the sample after hydrothermal treatment. After calcination at 450°C, the sample only contains titanium and oxygen elements (Fig. 2b), which proves that sodium ions have been removed [26].

Based on the above results, the growth mechanism of TiO₂ could be explained in the three steps. First, during the hydrothermal process, TBT reacted with NaOH solution and generated sodium titanate, so the hydrothermal product contained a large amount of sodium ions [27]. Then, the sodium ions in sodium titanate were replaced by hydrogen ions during the acid washing process. Finally, titanate acid was decomposed to TiO₂ after calcination. The whole process could be described by the following equations:

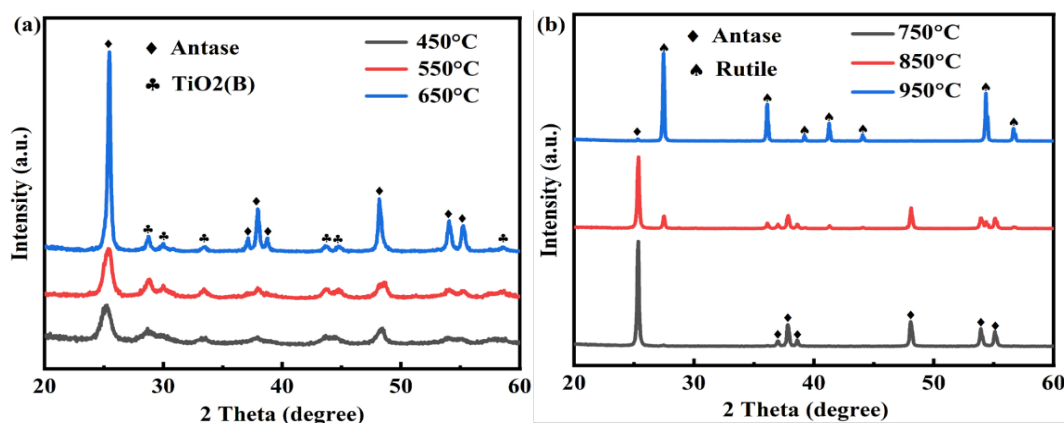
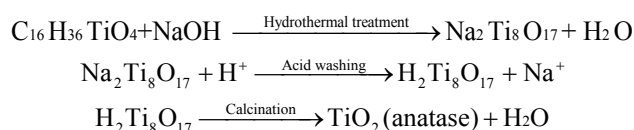


Fig. 3. XRD patterns of TiO₂ nanowires calcinated at different temperatures.

Fig. 3 shows the XRD patterns of the prepared samples with different calcination temperatures in air for 2 h. As can be seen in Fig. 3a, after calcination at 450 °C, 550 °C and 650 °C, TiO₂ is composed of anatase phase (JCPDS no. 21-1272) and TiO₂ (B) phase (JCPDS no. 29-1360) [28, 29]. Meanwhile, with the increase of calcination temperature, the peak intensity of anatase phase obviously increases, indicating the improvement of crystallinity. When the calcination temperature reaches 750 °C, only diffraction peaks of anatase TiO₂ phase could be observed (Fig. 3(b)). With further increase in the calcination temperature, rutile phase (JCPDS No. 21-1276) appears while the peak intensity of anatase TiO₂ decreases. Particularly, most of anatase phase disappears at 950 °C while the peak intensity of rutile phase increases greatly. The relative

content of rutile and anatase phase could be calculated from the formula [30]:

$$\chi = \frac{1}{1 + 0.8 \frac{I_A}{I_R}}$$

where χ is the mass fraction of rutile phase, I_A is the diffraction peak intensity of anatase phase (101), and I_R is the diffraction peak intensity of rutile phase (110). When the calcination temperature increases to 850 °C, nearly 16.6% anatase TiO₂ starts to transform to rutile phase. At 950 °C, most of the TiO₂ is rutile phase and the relative content of rutile and anatase are 98.1% and 1.9%, respectively.

3.2. Morphological characterization

Fig. 4 shows the SEM images of the TiO₂ samples calcined at various temperatures. As the calcination temperature below 650 °C, the surface morphology of TiO₂ nanowires has no great change. The average diameter of TiO₂ nanowires is about tens of nanometers and the length is around several micrometers. When the calcination temperature increases to 750 °C, a part of TiO₂ nanowires have been destroyed and aggregated to nanoparticles (Fig. 4d). With further increase in the calcination temperature to 850 °C, most of the nanowire structure has been collapsed and replaced by TiO₂ particles. At 950 °C, only TiO₂ particles with micrometer size can be found (Fig. 4f), which can be attributed to the phase transformation of anatase to rutile.

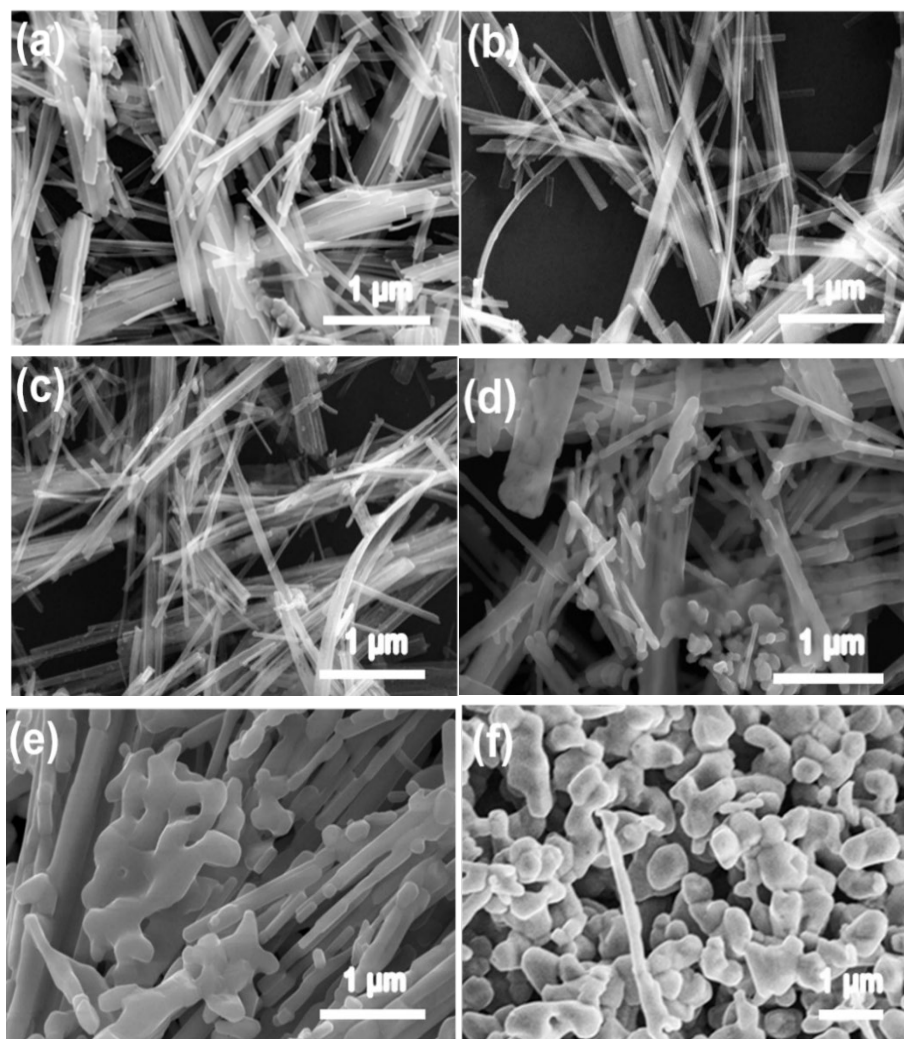


Fig. 4. SEM images of TiO₂ nanowires calcinated at different temperatures: (a)450 °C, (b)550 °C, (c)650 °C, (d)750 °C, (e)850 °C, (f)950 °C.

To obtain more specific information of the nanowires, TEM images of TiO_2 calcinated at 650°C were carried out. As shown in Fig. 5, TiO_2 displays the uniform wire structure with smooth surface. The length of the wire-like structure ranges from $2\ \mu\text{m}$ to $3\ \mu\text{m}$. The diameter of nanowires is about $25\ \text{nm}$.

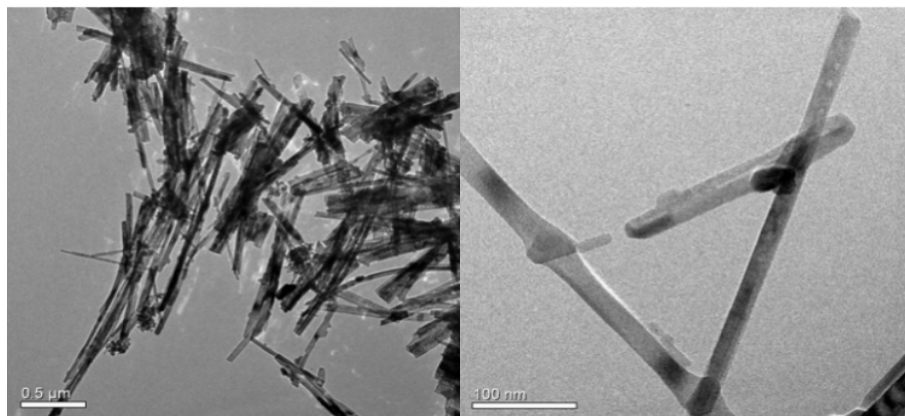


Fig. 5. TEM images of TiO_2 nanowires calcinated at 650°C .

3.3. Photocatalytic properties

The UV-vis absorption spectra of RhB dye solution over different TiO_2 photocatalysts are depicted in Fig. 6. It is clear that the intensity of absorption peaks of RhB decreases with increasing irradiation time, indicating the removal of dye. Notably, the absorbance of the RhB drops rapidly in the presence of TiO_2 catalyst calcinated at 650°C , and the absorbance is approximately a straight line after illumination for 60 min.

Fig. 7 compares the photocatalytic activity of different catalysts under the simulated solar light irradiation. It can be seen that the calcination temperature has a great effect on the photocatalytic activity of the TiO_2 . The photocatalytic efficiency of TiO_2 calcinated at 450°C and 550°C is 55.7% and 64.6%, respectively. The gradually improved photocatalytic efficiency of TiO_2 is due to the enhancement of crystallinity. TiO_2 nanowires calcinated at 650°C show superior photocatalytic degradation efficiency of 99.6%, which is attributed to the one-dimensional structure with good crystallinity and higher specific surface area, providing more active sites for photocatalytic reaction. Furthermore, the nanowire structure could provide efficient route for charge transfer and then reduce the combination of photogenerated electron-hole pairs, which promotes the improvement of degradation efficiency. However, when the calcination temperature continues to increase, the degradation efficiency decreases remarkably. The degradation efficiency is 68.3% for TiO_2 calcinated at 750°C while the removal efficiency is 29.7% at 850°C , which is ascribed to the transformation of anatase phase to rutile phase and the destruction of TiO_2 nanowires structure.

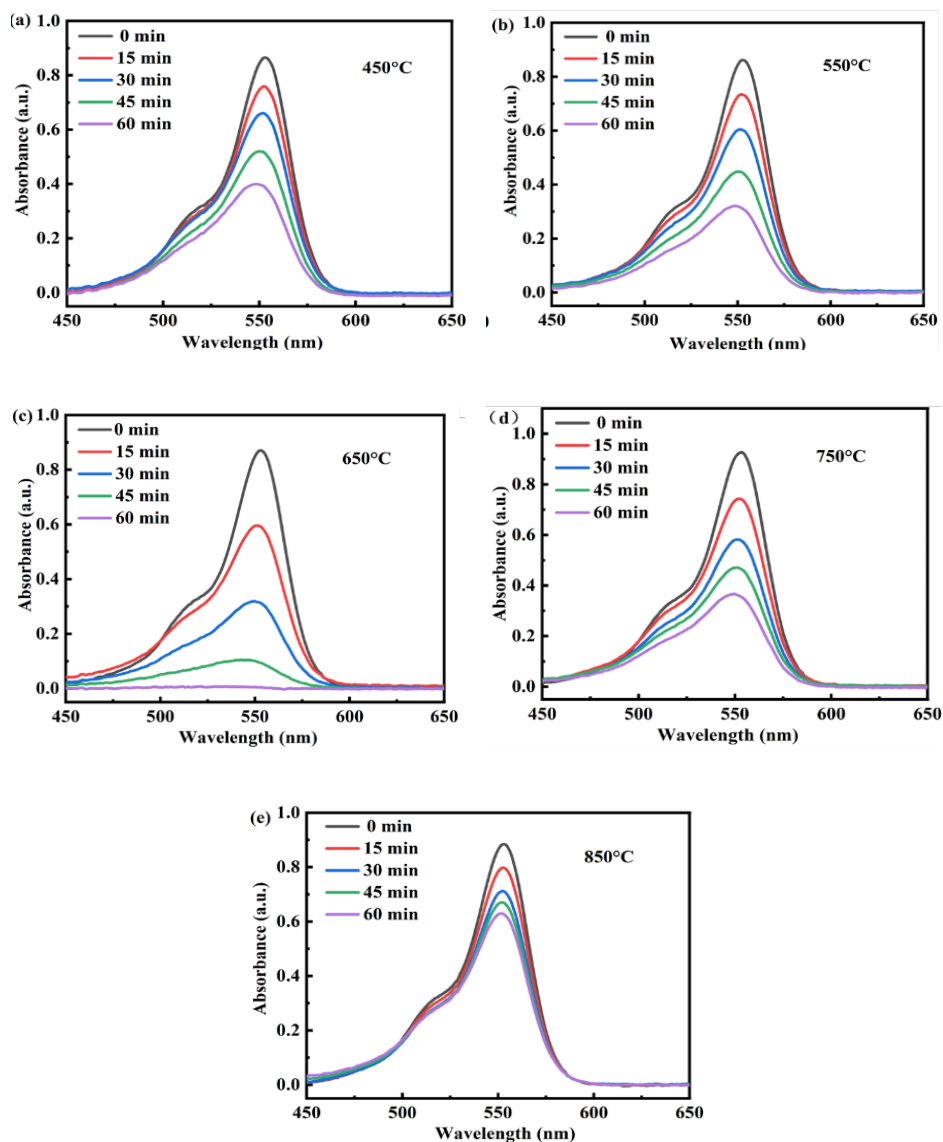


Fig. 6. Absorbance curves of RhB dye over the TiO_2 calcinated at various temperatures: (a) 450 °C, (b) 550 °C, (c) 650 °C, (d) 750 °C, (e) 850 °C.

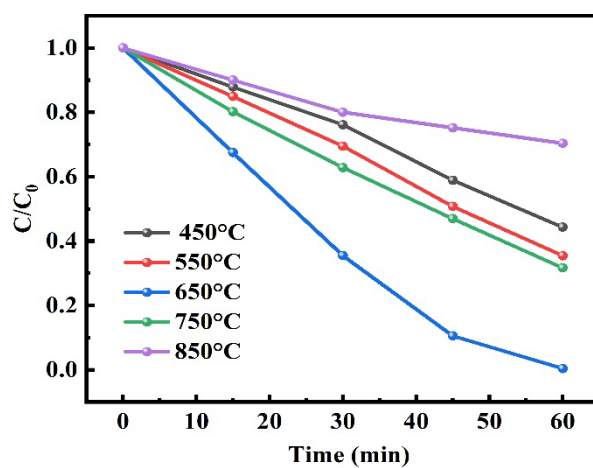


Fig. 7. Photocatalytic degradation efficiency of TiO_2 nanowires calcinated at different temperatures.

4. Conclusions

In summary, TiO₂ nanowires were prepared by hydrothermal treatment in NaOH solution using TBT as raw material. The growth mechanism of TiO₂ nanowires was proposed by analyzing the intermediate products after hydrothermal reaction and acid washing process. The effect of the calcination temperature on the crystal structure, surface morphology and photocatalytic performance of TiO₂ nanowires was investigated. TiO₂ nanowires calcined at 650 °C showed the highest photocatalytic degradation efficiency of 99.6%, which was attributed to the excellent crystal structure and the retainment of nanowires structure. With further increase in calcination temperature, the rutile phase appeared and the nanowire structure was destroyed, leading to the decrease of the photocatalytic activity.

Acknowledgments

This research is supported by the National Natural Science Foundation of China (No. 51702027).

References

- [1] H. M. Mousa, J. F. Alenezi, I. M. A. Mohamed, A. S. Yasin, A-F. M. Hashem, A. Abdal-hay, J. Alloy. Compd. 886, 161169 (2021); <https://doi.org/10.1016/j.jallcom.2021.161169>
- [2] T. Rungsawang, S. Sujinnapram, S. Nilphai, S. Wongrerkdee, Dig. J. Naomater. Bios. 16(4), 1209 (2021);
- [3] X. D. Zhu, Q. Zhou, Y. W. Xia, J. Wang, H. J. Chen, Q. Xu, J. W. Liu, W. Feng, S. H. Chen, J. Mater. Sci-Mater. El. 3216, 21511 (2021); <https://doi.org/10.1007/s10854-021-06660-5>
- [4] S. Fang, K. Lv, Q. Li, H. P. Ye, D. Y. Du, M. Li, Appl. Surf. Sci. 538, 336 (2015); <https://doi.org/10.1016/j.apsusc.2015.07.179>
- [5] Z. H. Zhang, S. Y. Zhai, M. H. Wang, H. F. Ji, L. H. He, C. M. Ye, C. B. Wang, S. M. Fang, H. Z. Zhang, J. Alloy. Compd. 659, 101 (2016); <https://doi.org/10.1016/j.jallcom.2015.11.027>
- [6] Q. R. Zhao, S. Y. Chen, B. H. Ren, S. N. Liu, Y. C. Zhang, X. Luo, W. Feng, Y. Sun, Opt. Mater. 135, 111987 (2023); <https://doi.org/10.1016/j.optmat.2022.113266>
- [7] H. B. Xia, X. T. Xu, D. Li, J. Alloy. Compd. 914, 165393 (2022); <https://doi.org/10.1016/j.jallcom.2022.165393>
- [8] A. S. Alkorbi, H. M. A. Javed, S. Hussain, S. Hussain, S. Latif, M. S. Mahr, M. S. Mustafa, R. Alsaiani, N. A. Alhemiary, Opt. Mater. 127, 112259 (2022); <https://doi.org/10.1016/j.optmat.2022.112259>
- [9] Y. Sun, S. Xu, J. Y. Zeng, S. S. Yang, Q. R. Zhao, Y. Yang, Q. Zhao, G. X. Wang, Dig. J. Naomater. Bios. 16(1), 239 (2021);
- [10] Y. Sun, Y. Gao, J. Y. Zeng, J. Guo, H. Wang, Mater. Lett. 279, 128506 (2020); <https://doi.org/10.1016/j.matlet.2020.128506>
- [11] X. H. Su, Q. Q. He, Y. E. Yang, G. Cheng, D. Dang, L. Yu, Diam. Relat. Mater. 114, 108168 (2021); <https://doi.org/10.1016/j.diamond.2020.108168>
- [12] E. Kim, K. H. Do, J. M. Wang, Y. Hong, A. P. Rangappa, D. A. Reddy, D. P. Kumar, T. K. Kim, Appl. Surf. Sci. 587, 152895 (2022); <https://doi.org/10.1016/j.apsusc.2022.152895>
- [13] J. Wang, Y. Zeng, L. L. Wan, J. Y. Zhao, J. Yang, J. Hu, F. F. Miao, W. T. Zhan, R. S. Chen, F. Liang, Appl. Surf. Sci. 509, 145301 (2020); <https://doi.org/10.1016/j.apsusc.2020.145301>
- [14] M. M. Zhang, C. R. Wang, H. Li, J. L. Wang, M. Li, X. S. Chen, Electrochim. Acta 326, 134972 (2019); <https://doi.org/10.1016/j.electacta.2019.134972>
- [15] M. V. Someswararao, R. S. Dubey, P. S. V. Subbarao, S. Singh, Results Phys. 11, 223 (2018); <https://doi.org/10.1016/j.rinp.2018.08.054>
- [16] Y. L. Zhang, C. S. Han, G. S. Zhang, D. D. Dionysiou, M. N. Nadagouda, Chem. Eng. J. 268, 170 (2015); <https://doi.org/10.1016/j.cej.2015.01.006>

- [17] D. Y. Wang, B. H. Ren, S. Y. Chen, S. N. Liu, W. Feng, Y. Sun, *Mater. Lett.* 330, 133229 (2023); <https://doi.org/10.1016/j.matlet.2022.133229>
- [18] Y. Sun, E. D. Liu, L. Zhu, Y. Wen, Q. W. Tan, W. Feng, *Dig. J. Naomater. Bios.* 14(2), 463 (2019);
- [19] Q. E. Zhao, W. Wen, Y. Xia, J. M. Wu, *J. Phys. Chem. Solids* 124, 192 (2019); <https://doi.org/10.1016/j.jpcs.2018.09.016>
- [20] R. Katal, S. Masudy-Panah, M. Tanhaei, M. H. D. A. Farahani, J. Y. Hu, *Chem. Eng. J.* 384, 123384 (2019); <https://doi.org/10.1016/j.cej.2019.123384>
- [21] C. S. Guo, J. X. Y. He, Y. Zhang, Y. Q. Wang, *Appl. Surf. Sci.* 257, 3798 (2011); <https://doi.org/10.1016/j.apsusc.2010.11.152>
- [22] W. Q. Qi, J. Du, Y. C. Peng, W. H. Wu, Z. J. Zhang, X. Y. Li, K. Li, K. Zhang, C. Gong, M. Luo, H. L. Peng, *Mater. Chem. Phys.* 207, 435 (2018); <https://doi.org/10.1016/j.matchemphys.2017.12.083>
- [23] J. Y. Liao, X. C. Xiao, D. Higgins, G. Lui, Z. W. Chen, *ACS. Appl. Mater. Inter.* 6(1), 568 (2014); <https://doi.org/10.1021/am4046487>
- [24] S. León-Ríos, R. E. González, S. Fuentes, E. C. Ángel, A. Echeverría, C. S. Demergasso, R. A. Zárate, *J. Nanomater.* 2016, (2016); <https://doi.org/10.1155/2016/7213672>
- [25] B. Santara, P. K. Giri, K. Imakita, M. Fujii, *Nanoscale* 5(12), 5476 (2013); <https://doi.org/10.1039/c3nr00799e>
- [26] M. Á. López Zavala, S. A. L. Morales, M. Ávila-Santos, *Heliyon* 3(11), (2017); <https://doi.org/10.1016/j.heliyon.2017.e00456>
- [27] A. S. Attar, Z. Hassani, *J. Mater. Sci. Technol.* 31(8), 828 (2015); <https://doi.org/10.1016/j.jmst.2014.12.010>
- [28] C. Y. Wang, X. F. Yu, X. H. Zhang, Z. M. Lu, X. X. Wang, X. P. Han, J. L. Zhao, L. L. Li, X. J. Yang, *J. Alloy. Compd.* 815, 152431 (2020); <https://doi.org/10.1016/j.jallcom.2019.152431>
- [29] L. A. Al-Hajji, A. A. Ismail, A. Al-Hazza, S. A. Ahmed, M. Alsaidi, F. Almutawa, A. Bumajdad, *J. Mol. Struct.* 1200, 127153 (2020); <https://doi.org/10.1016/j.molstruc.2019.127153>
- [30] X. D. Zhu, R. R. Zhu, L. X. Pei, H. Liu, J. Wang, W. Feng, Y. Jiao, W. M. Zhang, *J. Mater. Sci-Mater. El.* 30, 21210 (2019); <https://doi.org/10.1007/s10854-019-02494-4>